Journal of *Marine Science and Engineering*

MDPI

Article

An Updated Design Formula for Predicting the Compressive Strength of Plate: Elastic Buckling and Ultimate Compressive Strength

Do Kyun Kim [1,2,*,†], Hee Yeong Yang [1,†], Shen Li [3] and Seungjun Kim [4,*]

[1] Department of Naval Architecture and Ocean Engineering, College of Engineering, Seoul National University, Seoul 08826, Republic of Korea
[2] Research Institute of Marine Systems Engineering, Department of Naval Architecture and Ocean Engineering, Seoul National University, Seoul 08826, Republic of Korea
[3] Department of Naval Architecture, Ocean and Marine Engineering, University of Strathclyde, Glasgow G1 1XQ, UK
[4] School of Civil, Environmental and Architectural Engineering, Korea University, Seoul 02841, Republic of Korea
* Correspondence: do.kim@snu.ac.kr (D.K.K.); rocksmell@korea.ac.kr (S.K.)
† These authors contributed equally to this work.

Abstract: In the present study, a simplified and useful design formula is proposed to predict the ultimate strength of a plate under longitudinal compression. The shape of the elastic buckling strength (σ_{xE}) equation is utilised and adjusted to predict the ultimate compressive strength of the plate. In total, 600 cases of reasonable plate scenarios are selected to update the design formula by broadly considering the plate geometry (i.e., plate length, breadth, and thickness), material property (i.e., elastic modulus and yield strength), and initial deflection. The proposed formula, including the factor or coefficient for correction (C_f) may help ocean and shore (including onshore, offshore and nearshore) structural engineers improve safety and design the unstiffened plate element used in shipbuilding and oil and gas.

Keywords: limit state design; structural safety; update design formula; simply supported; Ocean and Shore Technology (OST)

Academic Editors: Erkan Oterkus and José António Correia

Received: 1 December 2024
Revised: 24 December 2024
Accepted: 8 January 2025
Published: 9 January 2025

Citation: Kim, D.K.; Yang, H.Y.; Li, S.; Kim, S. An Updated Design Formula for Predicting the Compressive Strength of Plate: Elastic Buckling and Ultimate Compressive Strength. *J. Mar. Sci. Eng.* **2025**, *13*, 113. https://doi.org/10.3390/jmse13010113

1. Introduction

Generally, plated structures utilised in ships and offshore structures are assembled by welding with various stiffeners to satisfy the required structural performance. As highlighted by Paik [1] and IACS [2], in recent years, the Ultimate Limit State Design (ULSD) approach has received increasing attention in structural design from Working Stress Design (WSD). Due to the predominant vertical bending moments on ocean mobilities, such as ships and ship-shaped offshore structures, the tertiary members (i.e., plates and stiffeners) that compose the mid-ship section of the ocean mobility are subjected to compressive and tensile loads. In particular, stiffened panels at the deck and bottom are severely exposed by axial loadings that are proportionate to their distance from the neutral axis. In the case of tension, as shown in Figure 1 (green-coloured line), it is often assumed that the material model maintains its yield strength after yield, which is typically Elastic Perfectly Plastic (EPP) or perfectly bi-linear behaviour, while in the case of compression, the prediction of ultimate strength performance, including buckling collapse characteristics, is important.

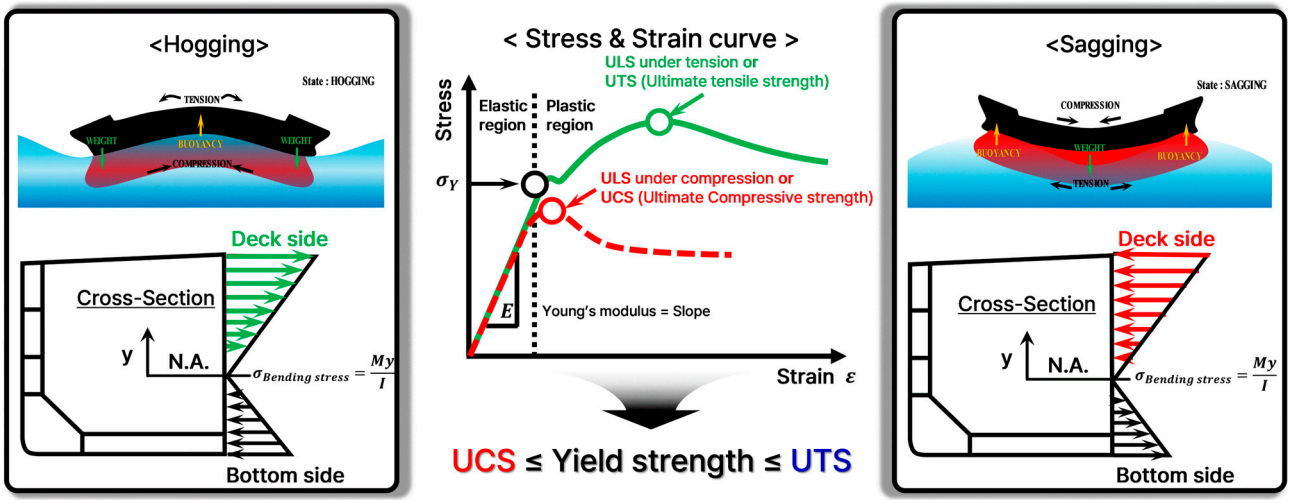

Figure 1. Explanation of ultimate limit state (ULS), including ultimate tensile strength (UTS) and ultimate compressive strength (UCS).

Regarding the ultimate compressive strength of the local elements, several studies have been conducted to investigate the collapse strength due to the compression being significantly lower than its expected strength (or yield strength), as shown in Figure 1 (red-coloured line). Historically, numerous studies have been carried out, and von Karman's elastic buckling strength of the plate equation, which adopts the effective width (b_e) concept, can be considered a significant improvement in technology development. This is a result of the two-dimensional (2D) element (plate or shell). There was also a significant development in the one-dimensional element (column), which was established much earlier than the 2D.

For 1D, the simplest but well-known approach is the elastic buckling force (P_E) or elastic buckling strength (σ_E) proposed by Euler. The well-known equations and detailed information can be referred to in Case I (Column buckling) and Case II (Plate buckling).

The well-known elastic buckling strength equation is summarised in Equation (1). In general, it is most commonly used for simple support conditions where the member is subjected to compression. In addition, it is characterised by the function of column slenderness ratio (λ) shown in Equation (1) and plate slenderness ratio (β) presented in Equation (2). An additional characteristic is that both of them (=slenderness ratios) are divided into geometric and material properties.

- Elastic buckling strength of the column (1D)

$$\sigma_{xE(column)} = \frac{P_E}{A} = \frac{\pi^2 EI}{AL^2} = \frac{\pi^2 E}{(A/I)L^2} = \frac{\pi^2 E}{(L/r)^2} = \frac{\sigma_Y}{\lambda^2} \tag{1}$$

$$where \quad \lambda = \sqrt{\frac{\sigma_Y}{\sigma_E}} = \underbrace{\frac{L}{\pi r}}_{Geometric} \times \underbrace{\sqrt{\frac{\sigma_Y}{E}}}_{Material}$$

- Elastic buckling strength of the plate (2D)

$$\sigma_{xE(plate)} = k_{x\ (plate)} \frac{\pi^2 E}{12(1-\nu^2)} \left(\frac{t}{b}\right)^2 = k_{x\ (plate)} \frac{\pi^2 D}{b^2 t} = k_{x\ (plate)} \frac{\pi^2}{12(1-\nu^2)} \left(\frac{1}{\beta^2}\right) \tag{2}$$

$$where \quad k_x = \left(\frac{mb}{a} + \frac{a}{mb}\right)^2, \ \beta = \underbrace{\frac{b}{t}}_{Geometric} \times \underbrace{\sqrt{\frac{\sigma_Y}{E}}}_{Material}, \ D = \frac{Et^3}{12(1-\nu^2)}$$

Based on the elastic buckling strength concept, various formulae have been progressively and continuously developed over time to take into account the phenomena that may occur in reality (i.e., imperfections, yield effects, residual stress effects, slenderness effects, and many others). These are often referred to as plasticity-corrected formulae, and the most commonly used formula in the International Association of the Classification Societies (IACS) is the Johnson–Ostenfeld (J-O) formula, as presented in Equation (3). This is one of the concepts that compensates for the limitations of the Euler or Elastic buckling strength formula, which overestimates the buckling capacity of structures in relatively small slenderness regions. The intention behind the formula is to ensure that the elastic buckling strength of a structure is always less than the yield strength if it exceeds 50% of the material yield strength which was derived from the Johnson parabola equation.

- Johnson–Ostenfeld (J-O) formula

$$\sigma_{cr(J-O)} = \begin{cases} \sigma_E & for\ \sigma_E \le 0.5\sigma_Y \\ \sigma_Y\left(1 - \frac{\sigma_Y}{4\sigma_E}\right) & for\ \sigma_E > 0.5\sigma_Y \end{cases} \tag{3}$$

Beyond the critical buckling strength (σ_{cr}), recent attempts have been made to develop limit a state-based (σ_u) structural safety assessment of structures. This basically adopts the effective width concept, as illustrated in Equation (4). For more information, the reader is recommended to refer to the ultimate limit state section of Paik's book [1].

$$\sigma_{xu} = \sigma_Y\left(\frac{b_e}{b}\right) \quad or \quad \frac{\sigma_{xu}}{\sigma_Y} = \frac{b_e}{b} \tag{4}$$

In this regard, a number of studies have been carried out to predict the ultimate compressive strength of structures. In particular, many studies have been carried out for plate elements or unstiffened panels [3–10] and stiffened plates or panels [11–25] under compression. In some cases, analytical solutions have been derived based on governing equations and relevant boundary conditions, but recent studies have also proposed empirical expressions in the form of curve fitting based on various parametric studies [8,26–30] as shown in the Figure 2. In particular, many empirical expressions include the slenderness ratio of plates and columns (Plate slenderness ratio, β and Column slenderness ratio, λ). As a typical example, the following equations have been developed for the empirical ultimate strength of plates (Equations (5a) to (5d)). A number of equations have also been developed for the compressive ultimate strength of stiffened panels (Equations (6a) to (6d)).

<Case I>: ULS of un-stiffened panel (= plate) in longitudinal compression: Typical example of the existing formulae.

- Faulkner [31]

$$\frac{\sigma_{xu}}{\sigma_Y} = \left\{ C_1/\beta - C_2/\beta^2 \quad for\ \beta \ge 1.0 \right. \tag{5a}$$

where C_1 = 2.0 and C_2 = 1.0 for the four-edge simply-supported condition, C_1 = 2.25 and C_2 = 1.25 for the four-edge clamped condition.

- Cui and Mansour [32]

$$\frac{\sigma_{xu}}{\sigma_Y} = \begin{cases} 1.0 & for\ \beta \le 1.9 \\ 0.08 + 1.09/\beta + 1.26/\beta^2 & for\ \beta > 1.9 \end{cases} \tag{5b}$$

- Paik et al. [33]

$$\frac{\sigma_{xu}}{\sigma_Y} = \begin{cases} -0.032\beta^4 + 0.002\beta^2 + 1 & for\ \beta \le 1.5 \\ 1.274/\beta & for\ 1.5 < \beta \le 3.0 \\ 1.248/\beta^2 + 0.283 & for\ \beta > 3.0 \end{cases} \quad (5c)$$

- Kim et al. [8]

$$\frac{\sigma_{xu}}{\sigma_Y} = 1 - e\left(\frac{c_1}{\beta} + \frac{c_2}{\beta^2} + \frac{c_3}{\beta^3} + c_4\right) \quad (5d)$$

where sub-coefficients (for c_1 to c_4) represent the amount of the initial deflection and can be referred to in Kim et al. [8].

< Case II > ULS of the stiffened panel in longitudinal compression: Typical example of the existing formulae.

- Paik and Thayamballi [34]

$$\frac{\sigma_{xu}}{\sigma_{Yeq.}} = \frac{1}{\sqrt{0.095 + 0.936\lambda^2 + 0.17\beta^2 + 0.188\lambda^2\beta^2 - 0.067\lambda^4}} \le \frac{1}{\sqrt{\lambda^2}} \quad (6a)$$

- Zhang and Khan [10]

$$\frac{\sigma_{xu}}{\sigma_{Yeq.}} = \frac{1}{\beta^{0.28}} \frac{1}{\sqrt{1 + \lambda^{3.2}}} \quad (6b)$$

- Kim et al. [30]

$$\frac{\sigma_{xu}}{\sigma_{Yeq.}} = \frac{1}{0.884 + e^{\lambda^2}} + \frac{1}{0.4121 + e^{\lambda^2}} \quad (6c)$$

- Kim et al. [28]

$$\frac{\sigma_{xu}}{\sigma_{Yeq.}} = \left[\begin{array}{l} c_0 + \left(c_1 + c_2\sqrt{\lambda} + \frac{c_3}{\beta} + c_4\frac{h_w}{t_w} + c_5\sqrt{\frac{I_{pz}}{I_{sz}}}\right)\sqrt{\lambda} \\ + \left(c_6 + \frac{c_7}{\beta} + c_8\frac{h_w}{t_w} + c_9\sqrt{\frac{I_{pz}}{I_{sz}}}\right)\frac{1}{\beta} \\ + \left(c_{10} + c_{11}\frac{h_w}{t_w} + c_{12}\sqrt{\frac{I_{pz}}{I_{sz}}}\right)\frac{h_w}{t_w} + \left(c_{13} + c_{14}\sqrt{\frac{I_{pz}}{I_{sz}}}\right)\sqrt{\frac{I_{pz}}{I_{sz}}} \end{array} \right] \le 1.0 \quad (6d)$$

where sub-coefficients for T-bar can be referred to in Kim et al. [28].

A detailed review of empirical equations for stiffeners can be found in Kim et al. [35]. However, the existing empirical formulae are still complex in terms of their shape, and it would be more effective if simple equations could be used to predict the ultimate strength performance. It is worth remembering that even very complex formulae can be analysed using deep learning techniques (ANN, DNN, many others) [36–44], but classification rules and design guidelines still favour simple formulae. In this regard, this study aims to propose a simplified empirical formula for predicting the ultimate strength performance of flat-plate elements used in ocean mobilities subjected to longitudinal compression. For simplification, the well-known elastic buckling strength expression for plates (Equation (2)) is utilised, and a new correction factor (C_f) is derived to estimate the compressive ultimate strength behaviour of plates by utilising k_x, which usually implies boundary condition effects. The results of this study are considered to be valuable data for evaluating the ultimate compressive strength performance of plate elements used in ocean mobilities.

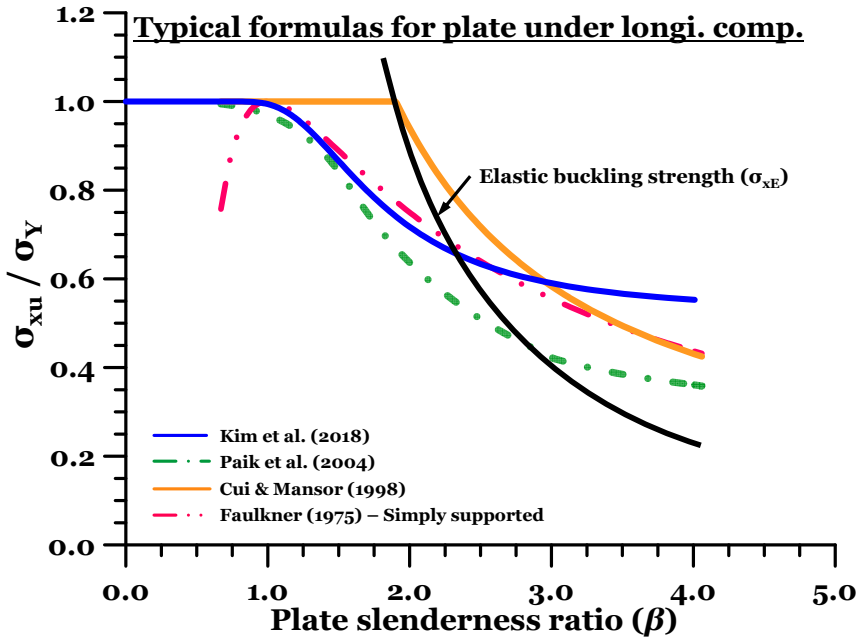

Figure 2. Comparison of the existing design formula for un-stiffened panel (plate element) [8,31–33].

2. Methodology

2.1. General

As mentioned earlier, the elastic buckling strength of the plate (σ_{xE}) under longitudinal compression can be predicted by Equation (3), and it can also be expressed by adding coefficient (C_f), as summarised in Equation (7).

$$ULS = \frac{\sigma_{xu}}{\sigma_Y} = \boxed{C_f} \times \underbrace{k_x \frac{\pi^2 E}{12(1-v^2)} \left(\frac{t}{b}\right)^2}_{\sigma_{xE}} \text{ or } \sigma_{xu} = \sigma_Y \boxed{C_f} \times \sigma_{xE} \quad (7)$$

where $k_x = \left(\frac{mb}{a} + \frac{a}{mb}\right)^2$, v = Poisson's ratio, t = plate thickness, b = plate width, E = material elastic modulus, C_f = coefficient to convert elastic buckling to ultimate compressive strength behaviours.

In particular, C_f, the main idea of this study, can consider the boundary conditions of the plate, the initial deflection amount, and have excellent scalability by considering the wide range of the plate slenderness ratios (=β, function of plate geometry and material property presented in Equation (2)). In addition, the relationship between the elastic buckling strength and the ultimate strength of the plate is compared and verified. Finally, various types of deflection shapes exist for the initial deflection, as stated by researchers [7,45,46]. However, the buckling mode shape-based initial deflection, which is most commonly used, was assumed. In reality, the initial deflection shape of the plate is complicated, i.e., hungry-horse mode, mountain mode, spoon mode, sinusoidal mode, buckling mode and others [45,47]. It means that the mode shape is not clear due to the welding [33]. However, when comparing the effects on ULS of the hungry-horse (HH) mode, Admiralty Research Establishment (ARE) mode, and critical buckling (CM) mode (represented by the sine wave) as recently investigated by shown in Shen et al. [48], it can be seen that the buckling mode provides the most conservative ULS estimates for the four specific grillage models. The situation reverses, however, when the initial deflection of the plate is smaller than the average level ($0.1\beta^2$t). Since the average level is generally assumed, it is considered logical to apply it in the present study. In this regard, we have included additional explanations in the manuscript.

The objectives of the present study are summarised as follows.

- To propose an empirical expression to predict the ultimate compressive strength of a plate and derive a correction factor (C_f) that can take into account initial deflection and different plate sizes.
- To verify the applicability of the developed empirical formula.
- To investigate the correlation between elastic buckling strength and the ultimate strength of a plate.

The results of this study (=updated formulae) are expected to help structural engineers predict the ultimate strength performance of plate elements used in ocean mobilities.

2.2. Development of the Correction Factor (C_f)

The overall figure for predicting the ultimate limit state (ULS) of the plate under longitudinal compression, including the correction factor (C_f) development procedure, is summarised in Figure 3.

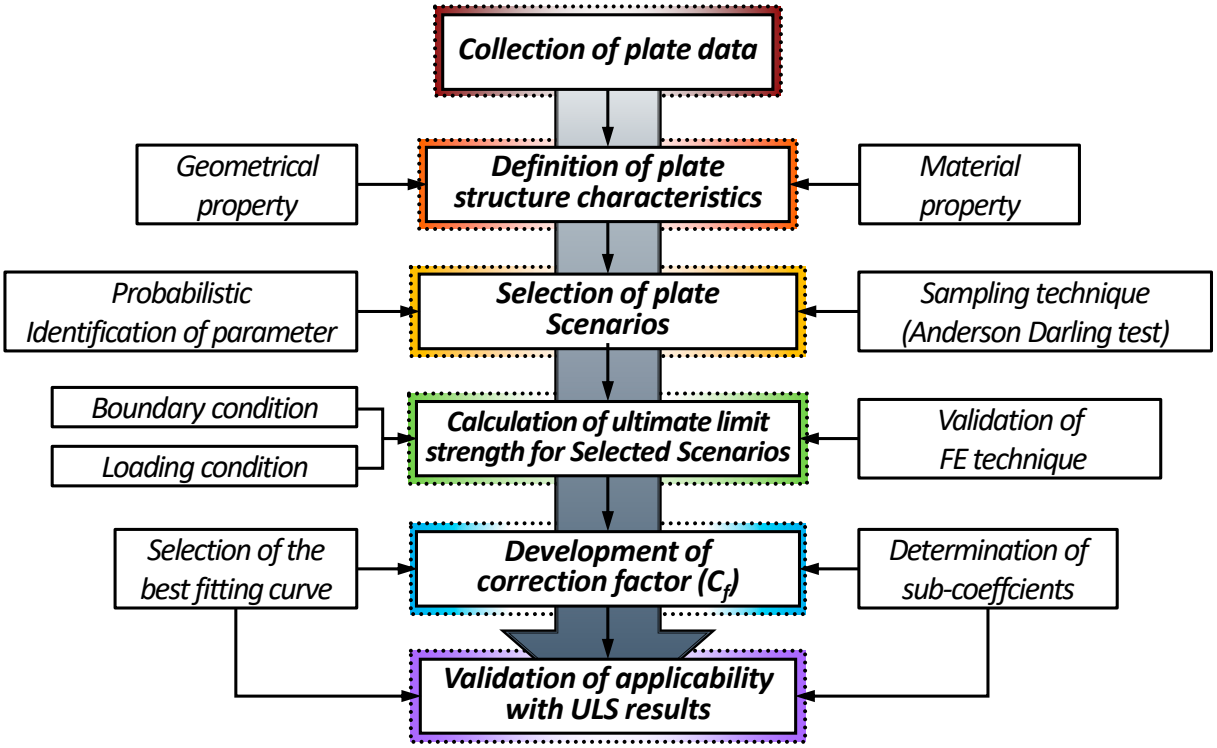

Figure 3. The procedure for the development of design formula, including correction factor in predicting ULS of a plate.

2.2.1. Collection of Plate Data and Definition of Plate Structure Characteristics

In the case of plates, 600 cases of plates were selected. In brief, the selection process was based on the results of Kim et al. [8], presented in Figure 4, which extracted the plate properties used in a total of 12 ships of various sizes, especially in the mid-ship section, and analysed their probabilistic characteristics. The geometries such as plate slenderness ratio, length (a, length), width (b, breadth), and thickness (t, thickness) are defined. In addition, material properties should also be defined. Poisson's ratio is typically assumed to be 0.3, and for elastic modulus (E), 205.8 GPa is applied in shipping industries. The material yield strength is one of the important factors where mild steel (σ_Y = 235 MPa) and high tensile steel (AH32 = 315 MPa) are generally used in shipyards. In this study, additional values of 355 MPa and 390 MPa were considered to investigate the material yield strength effect.

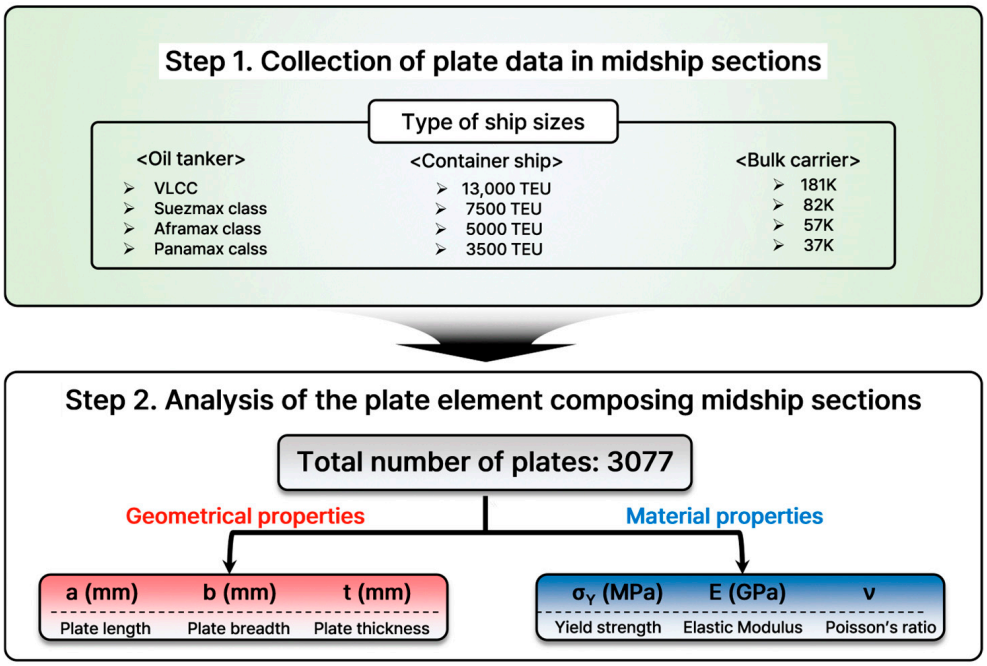

Figure 4. Explanation of selecting reliable scenarios of ship plate.

2.2.2. Selection of the Scenarios

As mentioned at the end of Section 2.2.1, an improved empirical formula is proposed in this study that can take into account both the effect of material yield strength and the initial deflection of the plate. In the case of the material model, we employed the Elastic Perfectly Plastic (EPP) model. The details of the selected scenarios can be referred to in Table 1.

Table 1. Summary of the analysis scenarios adopted.

Properties & Conditions		Number of Scenarios	Selected Scenarios
Geometric	Plate length (a)	1	4150mm
	Plate breadth (b)	1	830mm
	Plate thickness (t)	50	See Appendix A
Material	Yield strength (σ_Y)	4	235,315,355 and 390 MPa
	Elastic modulus	1	205.8 GPa
Initial imperfections	Initial deflection (C_{ID} = initial deflection coefficient)	3	0.025 (slight), 0.10 (average) and 0.30 (severe)
	Residual stress	N/A	N/A
Boundary condition		1	Simply-supported
Loading condition		1	Longitudinal compression
Total scenarios : $1 \times 1 \times 50 \times 4 \times 1 \times 3 \times 1 \times 1 = 600$ *cases*			

2.2.3. Calculation of Ultimate Limit Strength for Selected Scenarios

In this study, the ultimate strength characteristics of plate elements were obtained using a numerical method (= ANSYS nonlinear finite element analysis, NLFEA). It is recognised that there are various ways to predict structural behaviour, such as experimental, numerical, and analytical methods. Regarding the ultimate compressive strength behaviour of the plate and stiffened panels, several studies [49–56] have been conducted on the experimental method, and the numerical methods are widely adopted from the validation

results nowadays. One typical result can also be referred to in Kim et al. [5,57]. In their study, the ultimate compressive strength test of the curved plates was conducted and validated with the design formula.

The compressive load related to buckling collapse was applied. In the case of boundary condition (BC), the simply-supported BC was considered, as illustrated in Figure 5 (lefthand side), which enables the confirmation of the lowest structural capacity. Mesh size also plays an important role in FE analysis. A previous study by Kim et al. [58] recommended a number of elements (NoE = 10) in the plate width direction for flat plates and NoE = 20 or more for curved plates. Recently, Wang et al. [3] also provided relevant guidance to utilise the 3D solid element for ULS analysis. Since this study deals with flat plates, the NoE = 10 elements in plate width direction using 2D shell elements are reasonably applied, as shown in Figure 5. In the case of the initial deflection mode, the first buckling mode from the Eigen buckling analysis was utilised. Regarding the FE analysis technique, displacement control was used. It is also available to achieve the ULS from the load control option.

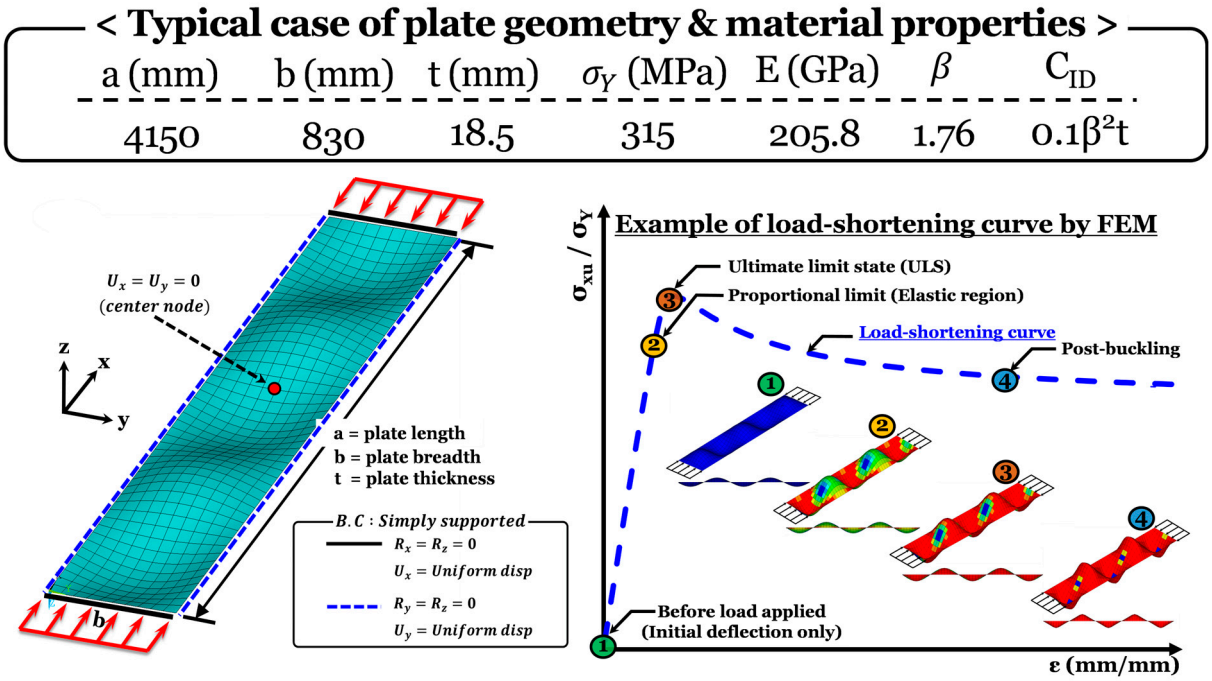

Figure 5. Example of load-shortening curve for the typical case.

The ULS data were collected from the selected scenario-based NLFEM, and the effect of the initial deflection amount was analysed by yield strength, as shown in Figure 6. It can be seen that the larger (=severe) the initial deflection amount, the lower the behaviour of ULS, regardless of the yield strength. It means that the initial deflection amount more significantly affects the ULS than material yield strength. In Equation (7), where C_f is the FEM data of the ULS on the left side, the right side can be calculated from the plate dimensions. Since simply-supported BC is only considered in this study, the value of k_x is considered to be 4.0. Figure 7 is a C_f versus plate slenderness ratio (β) diagram, as initial deflection amount and yield strength vary.

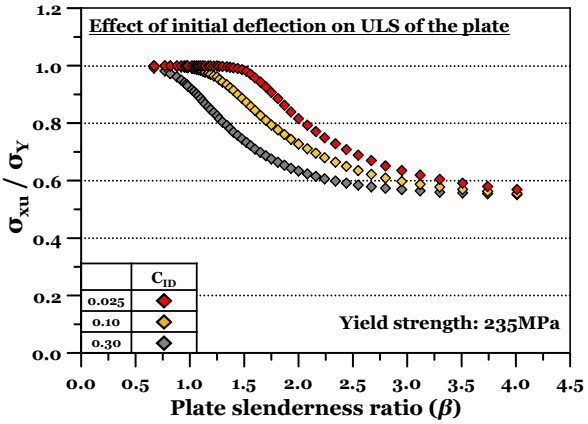

(**a**) Yield strength = 235 MPa.

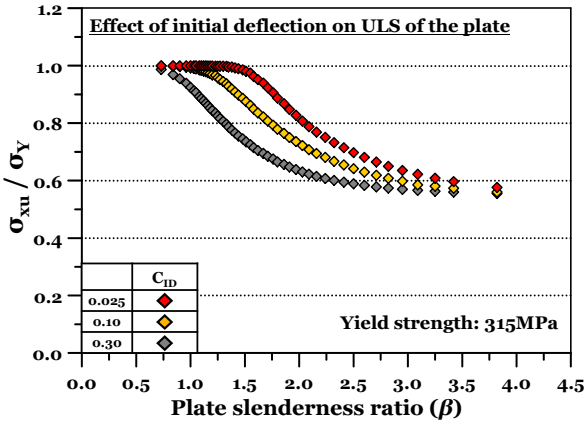

(**b**) Yield strength = 315 MPa.

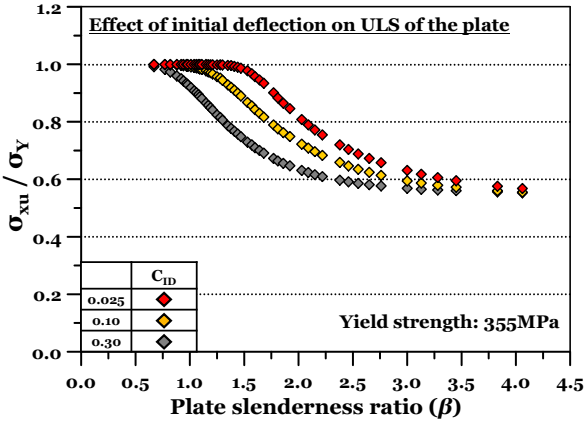

(**c**) Yield strength = 355 MPa.

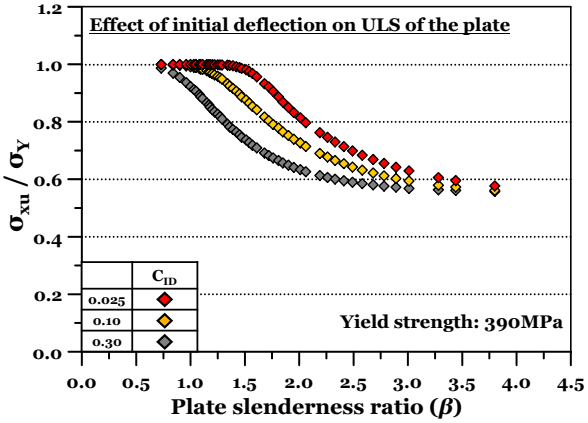

(**d**) Yield strength = 390 MPa.

Figure 6. Effect of initial deflection on ultimate limit strength of the plate.

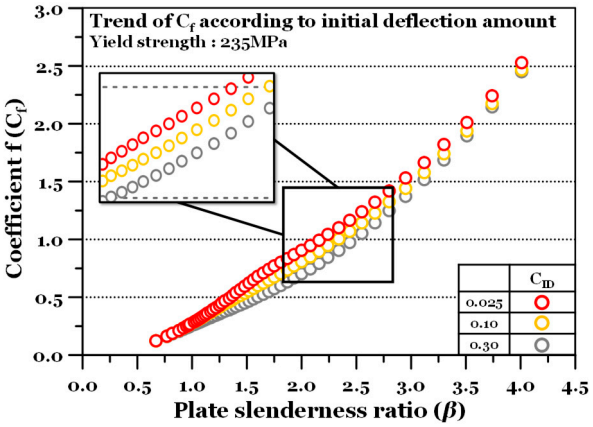

(**a**) Yield strength = 235 MPa.

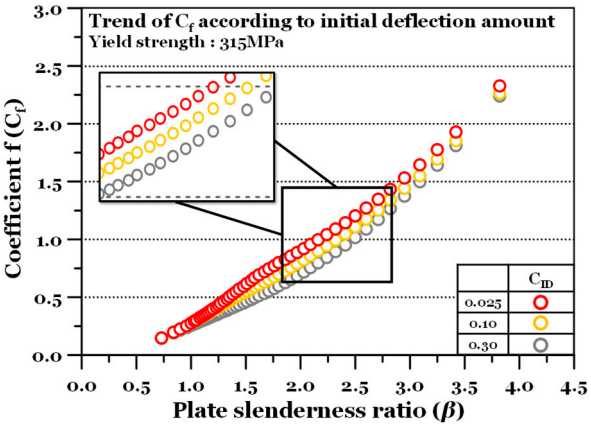

(**b**) Yield strength = 315 MPa.

Figure 7. *Cont.*

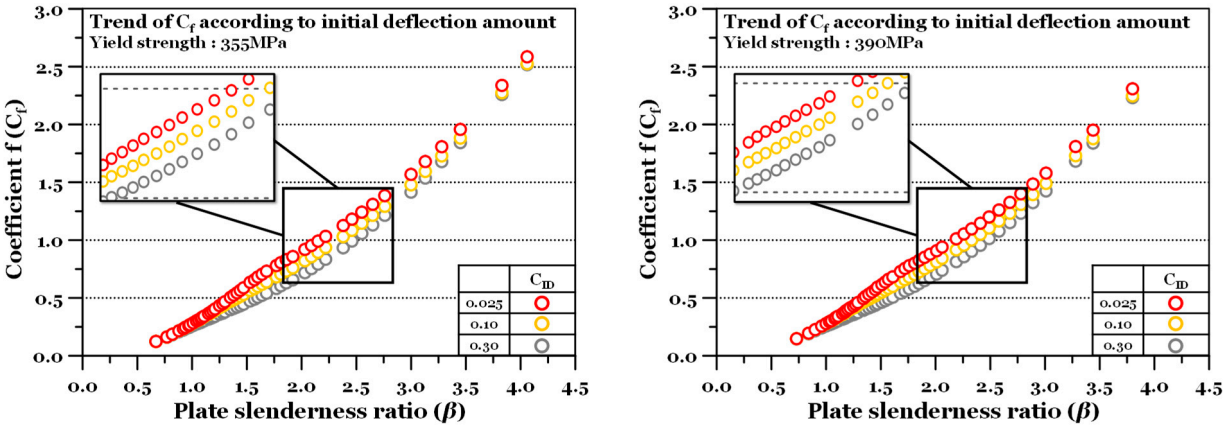

(**c**) Yield strength = 355 MPa. (**d**) Yield strength = 390 MPa.

Figure 7. Trend of C_f according to initial deflection amount.

2.2.4. Development of Correction Factor (or Sub-Equation) (C_f)

To calculate the coefficient C_f in Equation (7), the sub-equations were developed by regression analysis based on polynomial and logarithmic forms. From Figure 8, it can be seen that the behaviour of C_f changes around beta at 1.9. Several scholars, i.e., von Karman and Cui and Mansour, derived that a plate slenderness ratio of 1.9 is often considered to distinguish between thin and thick plates – for example, a thin plate when it is larger than 1.9 and a thick plate when it is smaller. Similarly, when analysing the present results, we also found that the tendency varies around the 1.9 threshold, which we used to develop the empirical formula.

It seems that the influence of the plate's ULS behaviour also affects the C_f trend. To ensure accuracy, correction factors (or sub-equations) (Equation (8)) were developed by dividing the ranges based on beta at 1.9. Table 2a,b summarise the coefficients obtained from the regression analysis according to the amount of initial deflection. To verify the accuracy, we calculated the statistical value of R^2 and confirmed its applicability (above 0.99 on average).

$$C_f = \begin{cases} f_1\beta^4 + f_2\beta^3 + f_3\beta^2 + f_4\beta + f_5 & for\ \beta < 1.9 \\ g_1\beta^{(g_2)} + g_3 & for\ \beta \geq 1.9 \end{cases} \quad (8)$$

where f_1 to f_5 = sub-coefficients for $\beta < 1.9$ (Table 2a) and g_1 to g_3 = sub-coefficients for $\beta \geq 1.9$ (Table 2b).

Table 2. (**a**) Obtained sub-coefficients from curve fitting ($\beta < 1.9$); (**b**) Obtained sub-coefficients from curve fitting ($\beta \geq 1.9$).

(a)

$\beta < 1.9$	Initial deflection amount (C_{ID})						
Sub-coefficients	0.025	0.05	0.10	0.15	0.20	0.25	0.30
f_1	−0.212	0.057	0.204	0.185	0.131	0.085	0.049
f_2	0.804	−0.518	−1.149	−0.967	−0.647	−0.385	−0.188
f_3	−0.846	1.447	2.341	1.844	1.165	0.637	0.252
f_4	0.684	−1.003	−1.515	−1.025	−0.452	−0.028	0.266
f_5	−0.154	0.293	0.394	0.236	0.070	−0.047	−0.124
R^2	0.999	0.999	0.999	0.999	0.999	0.999	0.999

Table 2. *Cont.*

(b)							
β ≥ 1.9	Initial deflection amount (C_{ID})						
Sub-coefficients	0.025	0.05	0.10	0.15	0.20	0.25	0.30
g_1	0.125	0.127	0.118	0.117	0.118	0.123	0.124
g_2	2.042	2.036	2.095	2.112	2.119	2.099	2.100
g_3	0.389	0.342	0.303	0.261	0.229	0.191	0.170
R^2	0.999	0.999	0.999	0.999	0.999	0.999	0.999

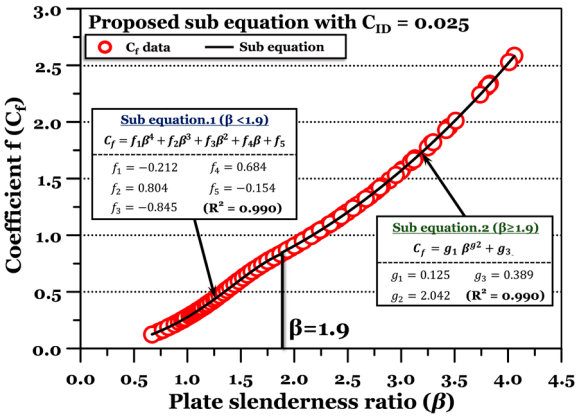

(**a**) Slight level ($w_{opl} = 0.025\beta^2 t$).

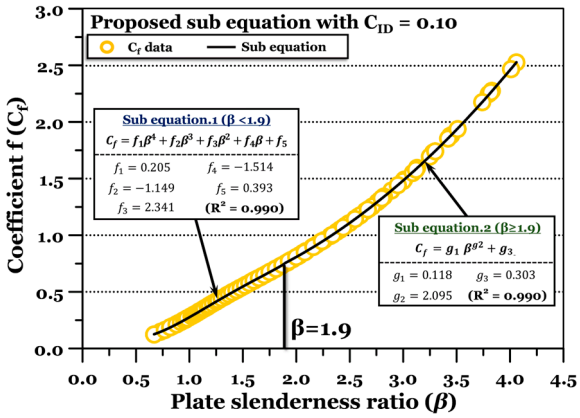

(**b**) Average level ($w_{opl} = 0.1\beta^2 t$).

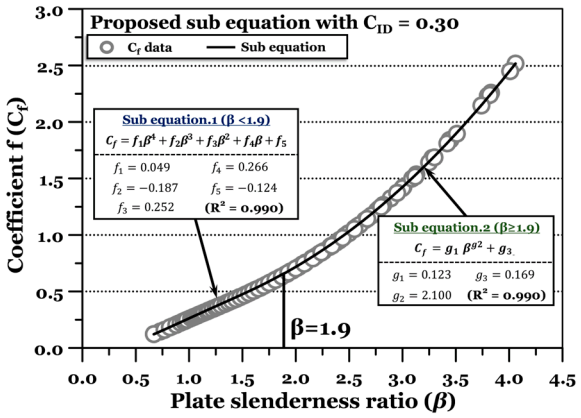

(**c**) Severe level ($w_{opl} = 0.3\beta^2 t$).

Figure 8. Development of correction factor (C_f) by determination of sub-coefficients and considering the initial deflection amount using the curve-fitting method.

2.2.5. Validation of the Correction Factor (C_f) Developed

Figure 9 presents the validation results of the ultimate strength predicted by the proposed formula in this study (Equation (9)) with the NLFEM analysis results. It can be seen from the mean values and coefficient of variation (COV) that the developed design formula predicts the compressive ultimate strength of the plate considering three initial deflection levels (0.025, 0.1 and $0.3\beta^2 t$) with good agreement. Figure 10 compares the ULS behaviour according to beta with different amounts of initial deflection.

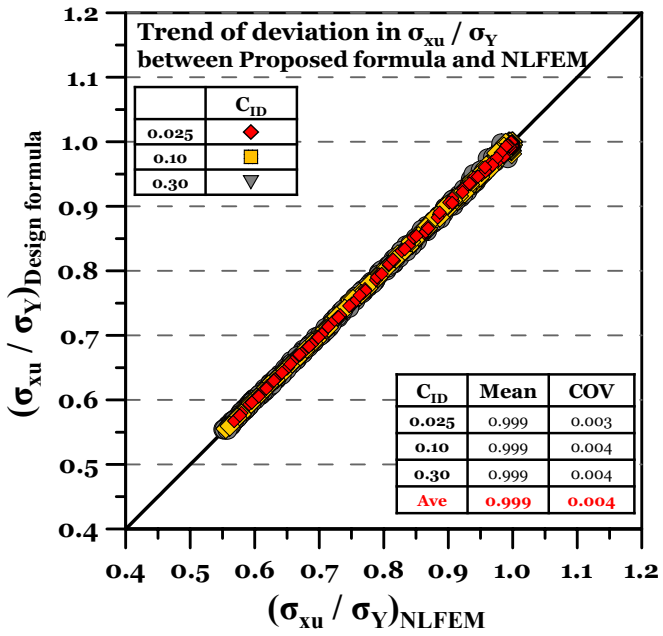

Figure 9. Trend of the deviation in the ultimate strength of plate between proposed update design formula and nonlinear-FEM (ANSYS).

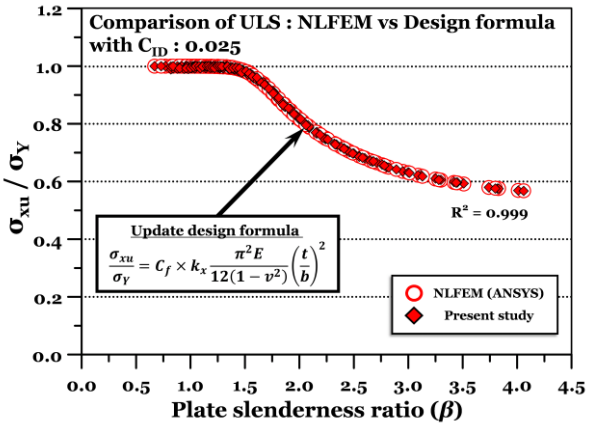

(**a**) Initial deflection: Slight level.

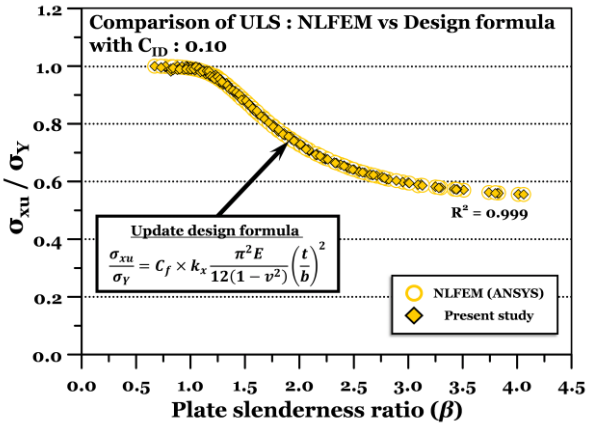

(**b**) Initial deflection: Average level.

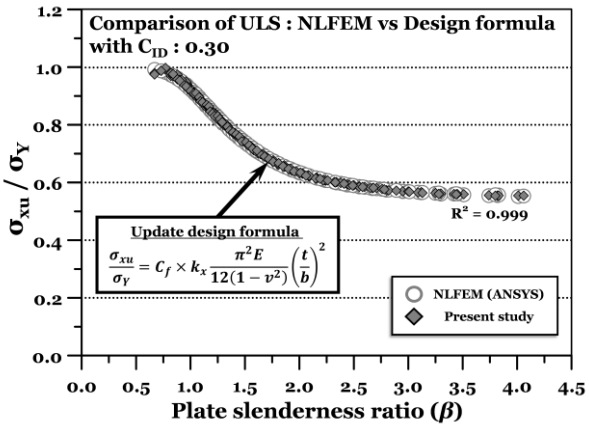

(**c**) Initial deflection: Severe level.

Figure 10. Comparison of NLFEM and proposed formula in this study for ultimate compressive strength of initially deflected plates.

- Proposed design formula

$$\frac{\sigma_{xu}}{\sigma_Y} = C_F \times \sigma_{xE} \tag{9}$$

where $\sigma_{xE} = k_x \frac{\pi^2 E}{12(1-v^2)} \left(\frac{t}{b}\right)^2$ = elastic buckling strength of the plate.

3. Discussions on the Proposed Design Formula (PROS and CONS)

The ultimate strength of the plate predicted by the updated design formula was compared with the elastic buckling strength calculated from Equation (3). Figure 11 shows the deviation of the ultimate compressive strength from the elastic buckling strength, and Figure 12 presents the comparison results by initial deflection.

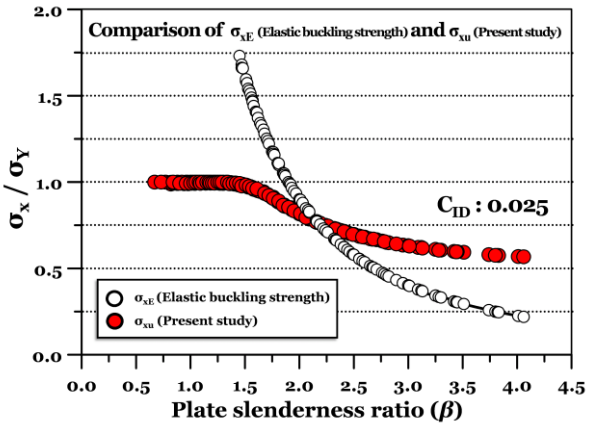

(**a**) Initial deflection: Slight level.

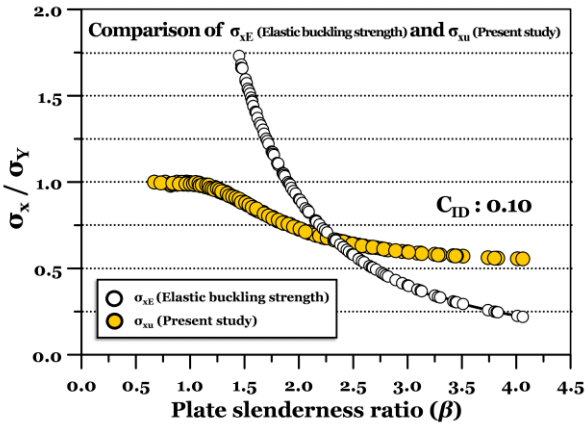

(**b**) Initial deflection: Average level.

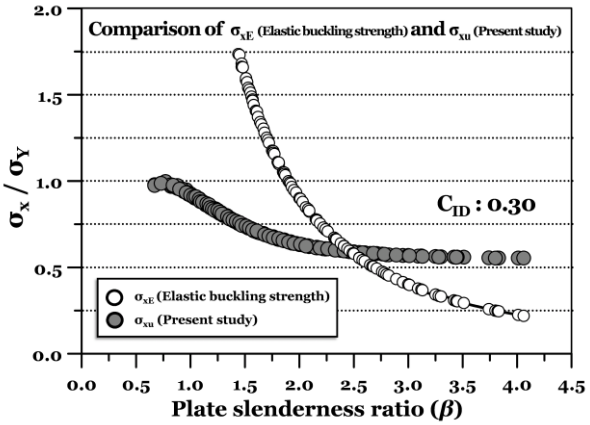

(**c**) Initial deflection: Severe level.

Figure 11. Comparison of σ_{xE} (elastic buckling strength) and σ_{xu} (ultimate compressive strength by the present study).

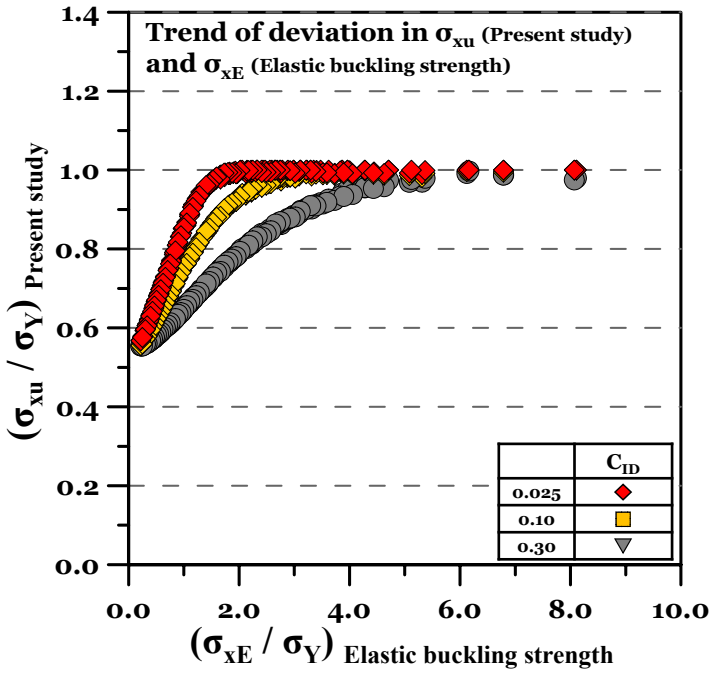

Figure 12. Trend of the deviation in σ_{xu} (present study) and σ_{xE} (elastic buckling strength).

Using the elastic buckling strength formula instead of the plastic correction Johnson–Ostenfeld equation, it was found that for a plate slenderness ratio (β) at 2.2 and below, the elastic buckling strength is on average 51.7% higher than the ultimate strength, while for β at 2.2 and above, the ultimate strength is on average 29.7% higher than the elastic buckling strength. Although the existing design criteria are based on the elastic zone, the safety margin should be accurately predicted because it directly relates to cost efficiency and safety. It is believed that the proposed formula enables the calculation of a more accurate structural capacity by utilising the elastic buckling strength and ultimate limit state, which can be calculated simultaneously with a simplified correction factor (or sub-equation C_f).

The obtained formula was compared with the NLFEM results and existing formulae, as shown in Figure 13. In the case of the Faulkner equation (Eq. 5a), ULS is set as 1.0 when the plate slenderness ratio (β) is less than 1.0, which means that the obtained ultimate compressive strength of the plate cannot exceed the material yield strength. One more thing here is that the proposed formula is based on the NLFEM results from the present study. This means that the other formulae are derived from the other datasets. For example, Kim et al. [8] proposed an advanced design formula for predicting the ULS of the plate under compression. They only considered two types of materials, i.e., mild steel and HT32 (yield strength = 235 and 315 MPa). In this study, we added two more materials, HT 36 and HT40, and mean and COV were slightly updated. It is important to clearly acknowledge the limitations of claiming superiority of empirical results obtained from one dataset over other formulae.

In addition, we can also consider the effect of the plate aspect ratio (=a/b or plate length/plate width) on the ultimate strength of the plate in longitudinal compression. In this study, we adopted a single value of the plate aspect ratio (a/b = 5.0), because the aspect ratio has less effect on the ULS of the plate as shown in Figure 14. If the aspect ratio (a/b) is not an integer, it is available to calculate the ULS by utilising the result that satisfies the nearest integer to that value. This may enable predicting the lowest ULS.

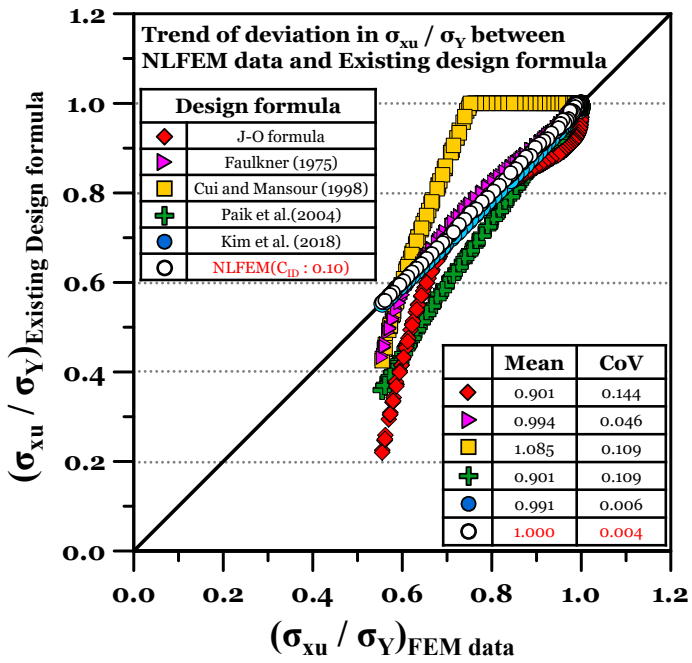

Figure 13. Statistical analysis results [2,8,31–33].

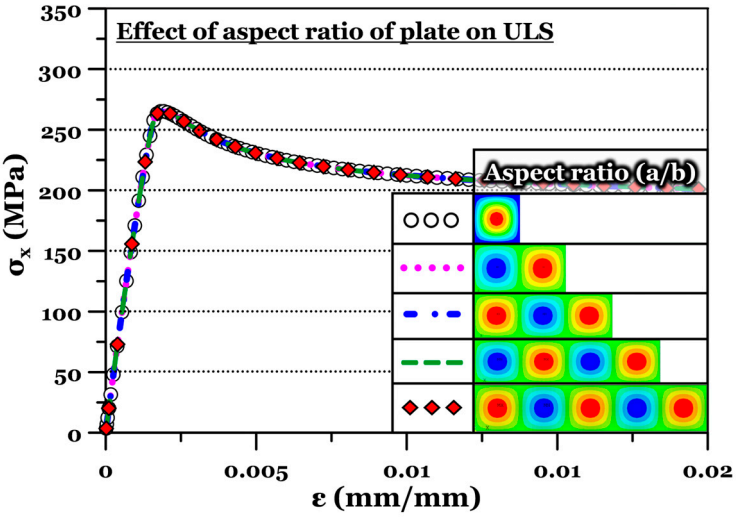

Figure 14. Effect of the plate aspect ratio on the ultimate limit state of the plate under longitudinal compression.

4. Conclusions and Limitations

In this study, the elastic buckling strength formula for plates was updated to include the initial deflection, boundary conditions and material yield strength of plates. In particular, Equation (7) represents the core of the present study, and the developed C_f is used to implement the various effects mentioned above. The results obtained in this study are summarised as follows.

- A design equation for predicting the ultimate compressive strength of plates was developed, which took the form of updating the elastic buckling strength equation. In particular, through the development of the C_f, an equation was developed that can take into account various conditions such as initial deflection and yield strength.
- The developed empirical formula showed an accuracy of $R^2 = 0.99$ compared to the results of nonlinear finite element analysis (NLFEA), which proves its applicability.

- The correlation between the elastic buckling strength and the ultimate strength of the plate was investigated. Compared to the elastic buckling strength, the compressive ultimate strength decreases as beta increases, with an average decrease of 29.7%. The details can be found in the developed C_f and ULS relationship. However, for thin plates with a large slenderness ratio, the ULS being greater than the elastic buckling strength is the background for introducing the ultimate strength criteria. Therefore, the percentage numbers many not be importantly considered.
- The applicable range of the plate slenderness ratio shall be clearly presented. As shown in Figure 15, it is recommended to utilise the proposed formula in the $0.067 \leq \beta$ range.

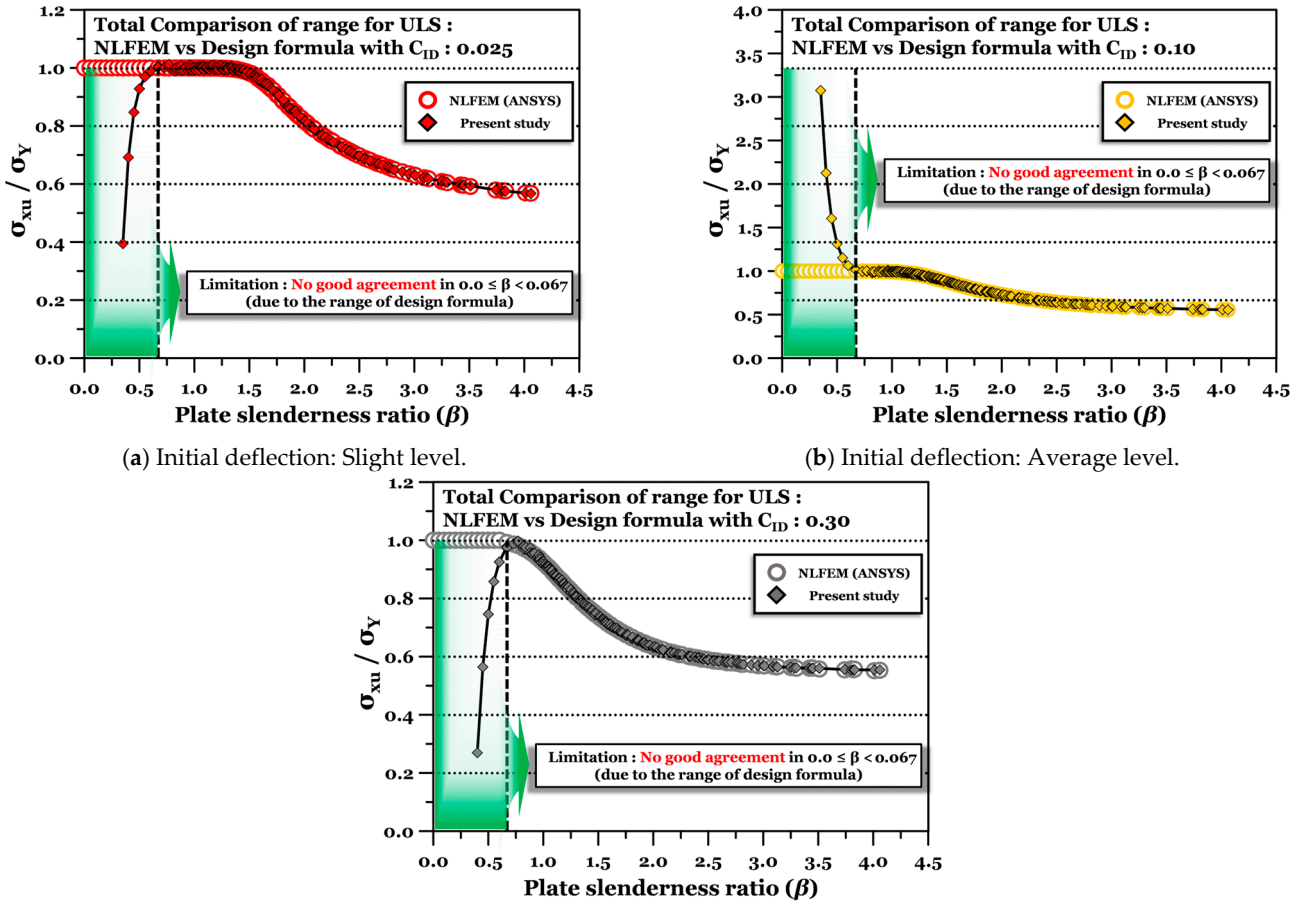

(**a**) Initial deflection: Slight level.

(**b**) Initial deflection: Average level.

(**c**) Initial deflection: Severe level.

Figure 15. Applicable range of the proposed formula.

This study conducted an in-depth investigation of the elastic buckling and ultimate compressive strength of a plate subjected to longitudinal compression. This is because it is the dominant load direction resulting from vertical bending motions on ocean mobilities (i.e., ships, ship-shaped offshore structures, and others). However, these structures are exposed to a variety of combined loads, and further research should be carried out on combined loading, along with lateral pressure, transverse compression, and shear. In addition, other boundary conditions should also be considered, which will be the subject of future research.

Author Contributions: Conceptualisation, D.K.K.; methodology, D.K.K., H.Y.Y., S.L. and S.K.; software, H.Y.Y.; validation, D.K.K. and S.L. and S.K.; formal analysis, D.K.K. and H.Y.Y.; investigation, D.K.K., H.Y.Y., S.L. and S.K.; resources, D.K.K.; writing—original draft preparation, D.K.K. and H.Y.Y.; writing—review and editing, D.K.K., S.L. and S.K.; visualisation, D.K.K. and H.Y.Y.; supervision,

D.K.K.; funding acquisition, D.K.K. All authors have read and agreed to the published version of the manuscript.

Funding: This research was supported by the Lloyd's Register Foundation (LRF, Grant No. CGY 100002). This research was conducted by the Ocean and Shore Technology (OST) research group (ost.snu.ac.kr) at Seoul National University.

Institutional Review Board Statement: Not applicable.

Informed Consent Statement: Not applicable.

Data Availability Statement: Data is contained within the article.

Conflicts of Interest: The authors declare no conflicts of interest.

Nomenclatures

A	=	Total area of stiffened panel
b	=	Breadth of plate, also taken as stiffener spacing
b_e	=	Effective width
D	=	Plate rigidity
E	=	Elastic modulus (GPa)
h_w	=	Height of web
I	=	Total moment of inertia of stiffener and plate
I_{pz}	=	Moment of inertia of plate in z-direction
I_{sz}	=	Moment of inertia of stiffener in z-direction
k_x	=	Buckling coefficient of plate which is determined depending on loading and boundary conditions
L	=	Length of stiffener (= length of plate)
k_x	=	Buckling coefficient of plate which is determined depending on loading and boundary conditions
P_E	=	Elastic buckling force
r	=	Radius of gyration
σ_E	=	Elastic buckling strength
σ_Y	=	Yield strength
σ_{Yeq}	=	Yield strength (equivalent)
t	=	Thickness of plate
t_w	=	Thickness of web
β	=	Plate slenderness ratio
λ	=	Column slenderness ratio

Appendix A

Table A1. Detailed plate scenarios.

No.	a(mm)	b(mm)	t(mm)	σ_Y(MPa)	E(GPa)	β
1	4150	830	42	235	205.8	0.67
2	4150	830	36.5	235	205.8	0.77
3	4150	830	34	235	205.8	0.82
4	4150	830	32	235	205.8	0.88
5	4150	830	30.5	235	205.8	0.92
6	4150	830	29.5	235	205.8	0.95
7	4150	830	29	235	205.8	0.97
8	4150	830	28.5	235	205.8	0.98
9	4150	830	27.5	235	205.8	1.02
10	4150	830	27	235	205.8	1.04

Table A1. *Cont.*

11	4150	830	26.5	235	205.8	1.06
12	4150	830	26	235	205.8	1.08
13	4150	830	25.5	235	205.8	1.10
14	4150	830	25	235	205.8	1.12
15	4150	830	24.5	235	205.8	1.14
16	4150	830	24	235	205.8	1.17
17	4150	830	23.5	235	205.8	1.19
18	4150	830	23	235	205.8	1.22
19	4150	830	22.5	235	205.8	1.25
20	4150	830	22	235	205.8	1.27
21	4150	830	21.5	235	205.8	1.30
22	4150	830	21	235	205.8	1.34
23	4150	830	20.5	235	205.8	1.37
24	4150	830	20	235	205.8	1.40
25	4150	830	19.5	235	205.8	1.44
26	4150	830	19	235	205.8	1.48
27	4150	830	18.5	235	205.8	1.52
28	4150	830	18	235	205.8	1.56
29	4150	830	17.5	235	205.8	1.60
30	4150	830	17	235	205.8	1.65
31	4150	830	16.5	235	205.8	1.70
32	4150	830	16	235	205.8	1.75
33	4150	830	15.5	235	205.8	1.81
34	4150	830	15	235	205.8	1.87
35	4150	830	14.5	235	205.8	1.93
36	4150	830	14	235	205.8	2.00
37	4150	830	13.5	235	205.8	2.08
38	4150	830	13	235	205.8	2.16
39	4150	830	12.5	235	205.8	2.24
40	4150	830	12	235	205.8	2.34
41	4150	830	11.5	235	205.8	2.44
42	4150	830	11	235	205.8	2.55
43	4150	830	10.5	235	205.8	2.67
44	4150	830	10	235	205.8	2.80
45	4150	830	9.5	235	205.8	2.95
46	4150	830	9	235	205.8	3.12
47	4150	830	8.5	235	205.8	3.30
48	4150	830	8	235	205.8	3.51
49	4150	830	7.5	235	205.8	3.74
50	4150	830	7	235	205.8	4.01
51	4150	830	44.5	315	205.8	0.73
52	4150	830	38.5	315	205.8	0.84
53	4150	830	36	315	205.8	0.90

Table A1. *Cont.*

No.	a(mm)	b(mm)	t(mm)	σ_Y(MPa)	E(GPa)	β
54	4150	830	34	315	205.8	0.96
55	4150	830	32.5	315	205.8	1.00
56	4150	830	31.5	315	205.8	1.03
57	4150	830	31	315	205.8	1.05
58	4150	830	30	315	205.8	1.08
59	4150	830	29.5	315	205.8	1.10
60	4150	830	29	315	205.8	1.12
61	4150	830	28.5	315	205.8	1.14
62	4150	830	28	315	205.8	1.16
63	4150	830	27.5	315	205.8	1.18
64	4150	830	27	315	205.8	1.20
65	4150	830	26.5	315	205.8	1.23
66	4150	830	26	315	205.8	1.25
67	4150	830	25.5	315	205.8	1.27
68	4150	830	25	315	205.8	1.30
69	4150	830	24.5	315	205.8	1.33
70	4150	830	24	315	205.8	1.35
71	4150	830	23.5	315	205.8	1.38
72	4150	830	23	315	205.8	1.41
73	4150	830	22.5	315	205.8	1.44
74	4150	830	22	315	205.8	1.48
75	4150	830	21.5	315	205.8	1.51
76	4150	830	21	315	205.8	1.55
77	4150	830	20.5	315	205.8	1.58
78	4150	830	20	315	205.8	1.62
79	4150	830	19.5	315	205.8	1.67
80	4150	830	19	315	205.8	1.71
81	4150	830	18.5	315	205.8	1.76
82	4150	830	18	315	205.8	1.80
83	4150	830	17.5	315	205.8	1.86
84	4150	830	17	315	205.8	1.91
85	4150	830	16.5	315	205.8	1.97
86	4150	830	16	315	205.8	2.03
87	4150	830	15.5	315	205.8	2.09
88	4150	830	15	315	205.8	2.16
89	4150	830	14.5	315	205.8	2.24
90	4150	830	14	315	205.8	2.32
91	4150	830	13.5	315	205.8	2.41
92	4150	830	13	315	205.8	2.50
93	4150	830	12.5	315	205.8	2.60
94	4150	830	12	315	205.8	2.71
95	4150	830	11.5	315	205.8	2.82

Table A1. *Cont.*

No.	a(mm)	b(mm)	t(mm)	σ_Y(MPa)	E(GPa)	β
96	4150	830	11	315	205.8	2.95
97	4150	830	10.5	315	205.8	3.09
98	4150	830	10	315	205.8	3.25
99	4150	830	9.5	315	205.8	3.42
100	4150	830	8.5	315	205.8	3.82
101	4150	830	51.5	355	205.8	0.67
102	4150	830	45	355	205.8	0.77
103	4150	830	42	355	205.8	0.82
104	4150	830	39	355	205.8	0.88
105	4150	830	37.5	355	205.8	0.92
106	4150	830	36.5	355	205.8	0.94
107	4150	830	35.5	355	205.8	0.97
108	4150	830	35	355	205.8	0.98
109	4150	830	34	355	205.8	1.01
110	4150	830	33	355	205.8	1.04
111	4150	830	32.5	355	205.8	1.06
112	4150	830	32	355	205.8	1.08
113	4150	830	31.5	355	205.8	1.09
114	4150	830	31	355	205.8	1.11
115	4150	830	30	355	205.8	1.15
116	4150	830	29.5	355	205.8	1.17
117	4150	830	29	355	205.8	1.19
118	4150	830	28.5	355	205.8	1.21
119	4150	830	27.5	355	205.8	1.25
120	4150	830	27	355	205.8	1.28
121	4150	830	26.5	355	205.8	1.30
122	4150	830	25.5	355	205.8	1.35
123	4150	830	25	355	205.8	1.38
124	4150	830	24.5	355	205.8	1.41
125	4150	830	24	355	205.8	1.44
126	4150	830	23.5	355	205.8	1.47
127	4150	830	22.5	355	205.8	1.53
128	4150	830	22	355	205.8	1.57
129	4150	830	21.5	355	205.8	1.60
130	4150	830	21	355	205.8	1.64
131	4150	830	20.5	355	205.8	1.68
132	4150	830	19.5	355	205.8	1.77
133	4150	830	19	355	205.8	1.81
134	4150	830	18.5	355	205.8	1.86
135	4150	830	18	355	205.8	1.92
136	4150	830	17	355	205.8	2.03
137	4150	830	16.5	355	205.8	2.09

Table A1. *Cont.*

No.	a(mm)	b(mm)	t(mm)	σ_Y(MPa)	E(GPa)	β
138	4150	830	16	355	205.8	2.15
139	4150	830	15.5	355	205.8	2.22
140	4150	830	14.5	355	205.8	2.38
141	4150	830	14	355	205.8	2.46
142	4150	830	13.5	355	205.8	2.55
143	4150	830	13	355	205.8	2.65
144	4150	830	12.5	355	205.8	2.76
145	4150	830	11.5	355	205.8	3.00
146	4150	830	11	355	205.8	3.13
147	4150	830	10.5	355	205.8	3.28
148	4150	830	10	355	205.8	3.45
149	4150	830	9	355	205.8	3.83
150	4150	830	8.5	355	205.8	4.06
151	4150	830	49.5	390	205.8	0.73
152	4150	830	43	390	205.8	0.84
153	4150	830	40	390	205.8	0.90
154	4150	830	37.5	390	205.8	0.96
155	4150	830	36	390	205.8	1.00
156	4150	830	35	390	205.8	1.03
157	4150	830	34.5	390	205.8	1.05
158	4150	830	33.5	390	205.8	1.08
159	4150	830	33	390	205.8	1.09
160	4150	830	32.5	390	205.8	1.11
161	4150	830	31.5	390	205.8	1.15
162	4150	830	31	390	205.8	1.17
163	4150	830	30.5	390	205.8	1.18
164	4150	830	30	390	205.8	1.20
165	4150	830	29.5	390	205.8	1.22
166	4150	830	29	390	205.8	1.25
167	4150	830	28.5	390	205.8	1.27
168	4150	830	28	390	205.8	1.29
169	4150	830	27	390	205.8	1.34
170	4150	830	26.5	390	205.8	1.36
171	4150	830	26	390	205.8	1.39
172	4150	830	25.5	390	205.8	1.42
173	4150	830	25	390	205.8	1.45
174	4150	830	24.5	390	205.8	1.47
175	4150	830	24	390	205.8	1.51
176	4150	830	23.5	390	205.8	1.54
177	4150	830	23	390	205.8	1.57
178	4150	830	22.5	390	205.8	1.61
179	4150	830	21.5	390	205.8	1.68

Table A1. *Cont.*

No.	a(mm)	b(mm)	t(mm)	σ_Y(MPa)	E(GPa)	β
180	4150	830	21	390	205.8	1.72
181	4150	830	20.5	390	205.8	1.76
182	4150	830	20	390	205.8	1.81
183	4150	830	19.5	390	205.8	1.85
184	4150	830	19	390	205.8	1.90
185	4150	830	18.5	390	205.8	1.95
186	4150	830	18	390	205.8	2.01
187	4150	830	17.5	390	205.8	2.06
188	4150	830	16.5	390	205.8	2.19
189	4150	830	16	390	205.8	2.26
190	4150	830	15.5	390	205.8	2.33
191	4150	830	15	390	205.8	2.41
192	4150	830	14.5	390	205.8	2.49
193	4150	830	14	390	205.8	2.58
194	4150	830	13.5	390	205.8	2.68
195	4150	830	13	390	205.8	2.78
196	4150	830	12.5	390	205.8	2.89
197	4150	830	12	390	205.8	3.01
198	4150	830	11	390	205.8	3.28
199	4150	830	10.5	390	205.8	3.44
200	4150	830	9.5	390	205.8	3.80

References

1. Paik, J.K. *Ship-Shaped Offshore Installations: Design, Construction, Operation, Healthcare and Decommissioning*, 2nd ed.; Cambridge University Press: Cambridge, UK, 2022.
2. IACS. *Common Structural Rules for Bulk Carriers and Oil Tankers*; International Association of Classification Societies: London, UK, 2022.
3. Wang, Z.; Kong, X.; Wu, W.; Li, S.; Kim, D.K. A guidance of solid element application in predicting the ultimate strength of flat plates in compression. *J. Ocean Eng. Sci.* **2024**, *in press*. [CrossRef]
4. Feng, L.; Yu, J.; Zheng, J.; He, W.; Liu, C. Experimental and numerical study of residual ultimate strength of hull plate subjected to coupled damage of pitting corrosion and crack. *Ocean Eng.* **2024**, *294*, 116710. [CrossRef]
5. Kim, J.-H.; Park, D.-H.; Kim, S.-K.; Kim, M.-S.; Lee, J.-M. Experimental Study and Development of Design Formula for Estimating the Ultimate Strength of Curved Plates. *Appl. Sci.* **2021**, *11*, 2379. [CrossRef]
6. Ahmadi, F.; Rahbar Ranji, A.; Nowruzi, H. Ultimate strength prediction of corroded plates with center-longitudinal crack using FEM and ANN. *Ocean Eng.* **2020**, *206*, 107281. [CrossRef]
7. Paik, J.K. *Ultimate Limit State Analysis and Design of Plated Structures*, 2nd ed.; John Wiley & Sons: Chichester, UK, 2018.
8. Kim, D.K.; Poh, B.Y.; Lee, J.R.; Paik, J.K. Ultimate strength of initially deflected plate under longitudinal compression: Part I = An advanced empirical formulation. *Struct. Eng. Mech.* **2018**, *68*, 247–259. [CrossRef]
9. Jiang, X.; Guedes Soares, C. A closed form formula to predict the ultimate capacity of pitted mild steel plate under biaxial compression. *Thin-Walled Struct.* **2012**, *59*, 27–34. [CrossRef]
10. Zhang, S.; Khan, I. Buckling and ultimate capability of plates and stiffened panels in axial compression. *Mar. Struct.* **2009**, *22*, 791–808. [CrossRef]
11. Wang, Z.; Kong, X.; Wu, W.; Kim, D.K. An advanced design diagram of stiffened plate subjected to combined in-plane and lateral loads considering initial deflection effects. *Thin-Walled Struct.* **2024**, *203*, 112144. [CrossRef]
12. Woloszyk, K.; Garbatov, Y.; Kowalski, J. Experimental ultimate strength assessment of stiffened plates subjected to marine immersed corrosion. *Appl. Ocean Res.* **2023**, *138*, 103679. [CrossRef]

13. Lee, H.H.; Kim, H.J.; Paik, J.K. Use of physical testing data for the accurate prediction of the ultimate compressive strength of steel stiffened panels. *Ships Offshore Struct.* **2023**, *18*, 609–623. [CrossRef]
14. Ringsberg, J.W.; Darie, I.; Nahshon, K.; Shilling, G.; Vaz, M.A.; Benson, S.; Brubak, L.; Feng, G.; Fujikubo, M.; Gaiotti, M.; et al. The ISSC 2022 committee III.1-Ultimate strength benchmark study on the ultimate limit state analysis of a stiffened plate structure subjected to uniaxial compressive loads. *Mar. Struct.* **2021**, *79*, 103026. [CrossRef]
15. Piculin, S.; Može, P. Ultimate resistance of longitudinally stiffened curved plates subjected to pure compression. *J. Constr. Steel Res.* **2021**, *181*, 106616. [CrossRef]
16. Zhang, S. A review and study on ultimate strength of steel plates and stiffened panels in axial compression. *Ships Offshore Struct.* **2016**, *11*, 81–91. [CrossRef]
17. Seo, J.K.; Song, C.H.; Park, J.S.; Paik, J.K. Nonlinear structural behaviour and design formulae for calculating the ultimate strength of stiffened curved plates under axial compression. *Thin-Walled Struct.* **2016**, *107*, 1–17. [CrossRef]
18. Tran, K.L.; Douthe, C.; Sab, K.; Dallot, J.; Davaine, L. Buckling of stiffened curved panels under uniform axial compression. *J. Constr. Steel Res.* **2014**, *103*, 140–147. [CrossRef]
19. Choi, B.H.; Hwang, M.O.; Yoon, T.Y.; Yoo, C.H. Experimental study of inelastic buckling strength and stiffness requirements for longitudinally stiffened panels. *Eng. Struct.* **2009**, *31*, 1141–1153. [CrossRef]
20. Li, D.; Chen, Z. Progressive collapse response and ultimate strength evaluation of stiffened plates with welding residual stress under combined biaxial cyclic loads and lateral pressure. *Mar. Struct.* **2025**, *99*, 103703. [CrossRef]
21. Li, D.; Chen, Z. Progressive collapse analysis and ultimate strength estimation of continuous stiffened panel under longitudinal extreme cyclic load and lateral pressure. *Ocean Eng.* **2023**, *285*, 115340. [CrossRef]
22. Hosseinabadi, O.F.; Khedmati, M.R. A review on ultimate strength of aluminium structural elements and systems for marine applications. *Ocean Eng.* **2021**, *232*, 109153. [CrossRef]
23. Paik, J.K.; Lee, D.H.; Noh, S.H.; Park, D.K.; Ringsberg, J.W. Full-scale collapse testing of a steel stiffened plate structure under cyclic axial-compressive loading. *Structures* **2020**, *26*, 996–1009. [CrossRef]
24. Manuel Gordo, J.; Guedes Soares, C. Compressive Tests on Long Continuous Stiffened Panels. *J. Offshore Mech. Arct. Eng.* **2011**, *134*, 021403. [CrossRef]
25. Khedmati, M.R.; Zareei, M.R.; Rigo, P. Empirical formulations for estimation of ultimate strength of continuous stiffened aluminium plates under combined in-plane compression and lateral pressure. *Thin-Walled Struct.* **2010**, *48*, 274–289. [CrossRef]
26. Kim, D.K.; Li, S.; Yoo, K.; Danasakaran, K.; Cho, N.-K. An empirical formula to assess ultimate strength of initially deflected plate: Part 2 = combined longitudinal compression and lateral pressure. *Ocean Eng.* **2022**, *252*, 111112. [CrossRef]
27. Kim, D.K.; Li, S.; Lee, J.R.; Poh, B.Y.; Benson, S.; Cho, N.-K. An empirical formula to assess ultimate strength of initially deflected plate: Part 1 = propose the general shape and application to longitudinal compression. *Ocean Eng.* **2022**, *252*, 111151. [CrossRef]
28. Kim, D.K.; Lim, H.L.; Yu, S.Y. Ultimate strength prediction of T-bar stiffened panel under longitudinal compression by data processing: A refined empirical formulation. *Ocean Eng.* **2019**, *192*, 106522. [CrossRef]
29. Xu, M.C.; Song, Z.J.; Zhang, B.W.; Pan, J. Empirical formula for predicting ultimate strength of stiffened panel of ship structure under combined longitudinal compression and lateral loads. *Ocean Eng.* **2018**, *162*, 161–175. [CrossRef]
30. Kim, D.K.; Lim, H.L.; Kim, M.S.; Hwang, O.J.; Park, K.S. An empirical formulation for predicting the ultimate strength of stiffened panels subjected to longitudinal compression. *Ocean Eng.* **2017**, *140*, 270–280. [CrossRef]
31. Faulkner, D. A Review of Effective Plating for Use in the Analysis of Stiffened Plating in Bending and Compression. *J. Ship Res.* **1975**, *19*, 1–17. [CrossRef]
32. Cui, W.; Mansour, A.E. Effects of welding distortions and residual stresses on the ultimate strength of long rectangular plates under uniaxial compression. *Mar. Struct.* **1998**, *11*, 251–269. [CrossRef]
33. Paik, J.K.; Thayamballi, A.K.; Lee, J.M. Effect of initial deflection shape on the ultimate strength behavior of welded steel plates under biaxial compressive loads. *J. Ship Res.* **2004**, *48*, 45–60. [CrossRef]
34. Paik, J.K.; Thayamballi, A.K. An Empirical Formulation For Predicting the Ultimate Compressive Strength of Stiffened Panels. In Proceedings of the The 7th International Offshore and Polar Engineering Conference (ISOPE 1997), Honolulu, HI, USA, 25–30 May 1997; ISOPE-I-97-444.
35. Kim, D.K.; Lim, H.L.; Yu, S.Y. A technical review on ultimate strength prediction of stiffened panels in axial compression. *Ocean. Eng.* **2018**, *170*, 392–406. [CrossRef]
36. Sivaprasad, H.; Lekkala, M.R.; Latheef, M.; Seo, J.; Yoo, K.; Jin, C.; Kim, D.K. Fatigue damage prediction of top tensioned riser subjected to vortex-induced vibrations using artificial neural networks. *Ocean. Eng.* **2023**, *268*, 113393. [CrossRef]
37. Zhao, Z.; Zhou, S.; Gao, H.; Liu, H. Predictions of compression capacity of randomly corroded spherical shells based on artificial neural network. *Ocean Eng.* **2022**, *257*, 111668. [CrossRef]
38. Park, Y.I.L.; Kim, J.-H. Artificial neural network based prediction of ultimate buckling strength of liquid natural gas cargo containment system under sloshing loads considering onboard boundary conditions. *Ocean Eng.* **2022**, *249*, 110981. [CrossRef]

39. Lee, D.; Lee, S.; Lee, J. Standardization in building an ANN-based mooring line top tension prediction system. *Int. J. Nav. Archit. Ocean Eng.* **2022**, *14*, 100421. [CrossRef]
40. La Ferlita, A.; Di Nardo, E.; Macera, M.; Lindemann, T.; Ciaramella, A.; Koulianos, N. A Deep Neural Network Method to Predict the Residual Hull Girder Strength. In Proceedings of the SNAME Maritime Convention, SMC 2022, Houston, TX, USA, 27–29 September 2022.
41. La Ferlita, A.; Di Nardo, E.; MacEra, M.; Lindemann, T.; Ciaramella, A.; Kaeding, P. Deep Neural Network (DNN) Method to Predict the Displacement Behavior of Neutral Axis for Ships in Vertical Bending. In *Technology and Science for the Ships of the Future, Proceedings of the 20th International Conference on Ship & Maritime Research, Genoa and La Spezia, Italy, 15–17 June 2022*; Progress in Marine Science and Technology; IOS Press: Amsterdam, The Netherlands, 2022; pp. 95–103.
42. Oh, D.; Race, J.; Oterkus, S.; Koo, B. Burst pressure prediction of API 5L X-grade dented pipelines using deep neural network. *J. Mar. Sci. Eng.* **2020**, *8*, 766. [CrossRef]
43. Remennikov, A.M.; Rose, T.A. Predicting the effectiveness of blast wall barriers using neural networks. *Int. J. Impact Eng.* **2007**, *34*, 1907–1923. [CrossRef]
44. Pu, Y.; Mesbahi, E. Application of artificial neural networks to evaluation of ultimate strength of steel panels. *Eng. Struct.* **2006**, *28*, 1190–1196. [CrossRef]
45. Kim, D.K.; Park, D.K.; Kim, J.H.; Kim, S.J.; Kim, B.J.; Seo, J.K.; Paik, J.K. Effect of corrosion on the ultimate strength of double hull oil tankers—Part I: Stiffened panels. *Struct. Eng. Mech. Int. J.* **2012**, *42*, 507–530. [CrossRef]
46. Li, S.; Georgiadis, D.G.; Kim, D.K.; Samuelides, M.S. A comparison of geometric imperfection models for collapse analysis of ship-type stiffened plated grillages. *Eng. Struct.* **2022**, *250*, 113480. [CrossRef]
47. Paik, J.K.; Thayamballi, A.K. *Ultimate Limit State Design of Steel-Plated Structures*; Wiley: New York, NY, USA, 2003.
48. Li, S.; Kim, D.K.; Benson, S. The influence of residual stress on the ultimate strength of longitudinally compressed stiffened panels. *Ocean Eng.* **2021**, *231*, 108839. [CrossRef]
49. ISSC. Ultimate Strength (Committee III.1). In Proceedings of the 15th International Ship and Offshore Structures Congress (ISSC 2003), San Diego, CA, USA, 11–15 August 2003.
50. ISSC. Ultimate Strength (Committee III.1). In Proceedings of the 16th International Ship and Offshore Structures Congress (ISSC 2006), Southampton, UK, 20–25 August 2006.
51. ISSC. Ultimate Strength (Committee III.1). In Proceedings of the 17th International Ship and Offshore Structures Congress (ISSC 2009), Seoul, Republic of Korea, 16–21 August 2009.
52. ISSC. Ultimate Strength (Committee III.1). In Proceedings of the 18th International Ship and Offshore Structures Congress (ISSC 2012), Rostock, Germany, 9–13 September 2012.
53. ISSC. Ultimate Strength (Committee III.1). In Proceedings of the 19th International Ship and Offshore Structures Congress (ISSC 2015), Cascais, Portugal, 7–10 September 2015.
54. ISSC. Ultimate Strength (Committee III.1). In Proceedings of the 20th International Ship and Offshore Structures Congress (ISSC 2018), Liège, Belgium and Amsterdam, The Netherlands, 9–14 September 2018.
55. ISSC. Ultimate Strength (Committee III.1). In Proceedings of the 21st International Ship and Offshore Structures Congress (ISSC 2022), Vancouver, BC, Canada, 11–15 September 2022.
56. ISSC. Ultimate Strength (Committee III.1). In Proceedings of the 22nd International Ship and Offshore Structures Congress (ISSC 2025), Wuxi, China, 22–26 September 2025.
57. Kim, D.K.; Wong, A.M.K.; Hwang, J.; Li, S.; Cho, N.-K. A novel formula for predicting the ultimate compressive strength of the cylindrically curved plates. *Int. J. Nav. Archit. Ocean Eng.* **2024**, *16*, 100562. [CrossRef]
58. Kim, D.K.; Ban, I.; Poh, B.Y.; Shin, S.-C. A useful guide of effective mesh-size decision in predicting the ultimate strength of flat- and curved plates in compression. *J. Ocean. Eng. Sci.* **2023**, *8*, 401–417. [CrossRef]